Received: 29 May 2021 | Revised: 13 September 2021 | Accepted: 18 September 2021

DOI: 10.1111/cas.15151

Cancer Science WILEY

ORIGINAL ARTICLE

G protein pathway suppressor 2 suppresses gastric cancer by destabilizing epidermal growth factor receptor

Yuan Si[1,2,3] | Haitao Zhang[4] | Peng Peng[1,3,5] | Chu Zhu[4] | Jie Shen[1,3] | Yilian Xiong[1,3] | Xuewen Liu[1,5] | Yuchen Xiang[1,3,5] | Wenjuan Li[1,3] | Yuliang Ren[1,3] | Fang Wan[1,3] | Liang Zhang[1,3,5] | Ying Liu[1,2,3,5]

[1]Laboratory of Molecular Targeted Therapy of Cancer, Institute of Basic Medical Sciences, Hubei University of Medicine, Shiyan, China

[2]Hubei Key Laboratory of Wudang Local Chinese Medicine Research, Hubei University of Medicine, Shiyan, China

[3]Hubei Key Laboratory of Embryonic Stem Cell Research, Hubei University of Medicine, Shiyan, China

[4]Sir Run Run Shaw Hospital, School of Medicine, Zhejiang University, Hangzhou, China

[5]Laboratory of Molecular Targeted Therapy of Cancer, Biomedical Research Institute, Hubei University of Medicine, Shiyan, China

Correspondence
Ying Liu and Yuan Si, Laboratory of Molecular Targeted Therapy of Cancer, Institute of Basic Medical Sciences, Hubei University of Medicine, 30 South Renmin Road, Shiyan, Hubei 442000, China.
Email: ying_liu1002@163.com (Y. L.); siyuan138@126.com (Y. S.)

Funding information
National Natural Science Foundation of China, Grant/Award Number: 82072928 and 81802387; Department of Science and Technology, Hubei Provincial People's Government, Grant/Award Number: 2021CFA071; Hubei Provincial Department of Education, Grant/Award Number: T201915

Abstract

G protein pathway suppressor 2 (GPS2) is expressed in most human tissues, including the stomach. However, the biological functions of GPS2 in cancer, as well as the underlying molecular mechanisms, remain poorly understood. Here, we report that GPS2 expression was aberrantly downregulated in gastric cancer (GC) tissues compared with control tissues. Clinicopathologic analysis showed that low GPS2 expression was significantly correlated with pathological grade, lymph node stage, and invasive depth. Kaplan-Meier analysis indicated that patients with low GPS2 expression showed poorer overall survival rates than those with high GPS2 expression. Moreover, GPS2 overexpression decreased GC cell proliferation, colony formation, tumorigenesis, and invasion. Overexpression of GPS2 reduced the protein expression of epidermal growth factor receptor (EGFR) and inhibited its downstream signaling in GC cells. Interestingly, GPS2 decreased EGFR protein expression, which was reversed by a lysosome inhibitor. Furthermore, GPS2 reduced EGFR protein stability by enhancing the binding of EGFR and an E3 ligase, c-Cbl, which promoted the ubiquitination of EGFR, ultimately leading to its degradation through the lysosomal pathway. Further analysis indicated that GPS2 activated autophagy and promoted the autophagic flux by destabilizing EGFR. Taken together, these results suggest that low GPS2 expression is associated with GC progression and provide insights into the applicability of the GPS2-EGFR axis as a potential therapeutic target in GC.

KEYWORDS
autophagy, c-Cbl, EGFR, gastric cancer, GPS2

Abbreviations: AO, acridine orange; c-Cbl, Casitas B-lineage lymphoma; CHX, cycloheximide; EEA1, early endosome antigen 1; EGF, epidermal growth factor; EGFR, epidermal growth factor receptor; GC, gastric cancer; GPS2, G protein pathway suppressor 2; HCQ, hydroxychloroquine; IHC, immunohistochemistry; LAMP-1, lysosomal associated membrane protein 1; LC3, microtubule-associated protein 1 light chain 3; NC, nonspecific control; NCE, non-clathrin-mediated endocytosis; NCOR, Nuclear Receptor Co-Repressor; qPCR, quantitative PCR; RTK, receptor tyrosine kinase; TCGA, The Cancer Genome Atlas; TCGA-STAD, The Cancer Genome Atlas of Stomach Adenocarcinoma; TMA, tissue microarray.

1 | INTRODUCTION

Gastric cancer is the sixth most common malignancy in the world and the third leading cause of cancer-related deaths; therefore, GC contributes significantly to the global burden of cancer. Although the global incidence and mortality rates of GC have significantly decreased over the past 50 years, GC still has one of the highest incidences in East Asian countries.[1] The incidence and mortality rates of GC in China are second only to those of lung cancer. The incidence and mortality rates of GC are highest in rural areas.[2] Due to the lack of effective biomarkers for the early detection of GC and the prediction of its chemosensitivity and recurrence rates, the outcome of GC patients remains unsatisfactory. As no obvious characteristic symptoms are observed in the early stage of the disease, GC is not easy to detect, and the pain it causes is ignored if it is not severe. Therefore, GC is often diagnosed in the advanced stage, and the treatment efficacy is poor. Diagnosis usually occurs too late to allow for effective treatment, resulting in a 5-year survival rate of less than 20%.[3] New therapies targeting specific molecules should be developed to improve the clinical outcome of GC.

Endocytosis begins with the internalization of plasma membrane cargo into early endosomes. These vesicles can mature into endosomes and further mature into various cell compartments, including circulating endosomes (fused with plasma membrane) or late endosomes (fused with lysosome), thereby regulating the circulation or degradation of endocytic cargo such as RTK.[4,5] Epidermal growth factor receptor is a member of the c-erbB family RTK and is highly expressed and activated in a variety of human tumors, including GC.[6] Abnormal activation of EGFR is an important step in the malignant transformation of cancer cells and the progression of tumors. Activation of EGFR, in turn, activates its downstream kinases, such as AKT and ERK, thereby promoting cancer cell proliferation, invasion, and apoptosis resistance.[7,8] The binding of EGF to EGFR not only activates signals downstream of EGFR but also stimulates the rapid internalization of EGFR. EGFR-mediated cell signaling and its endocytosis are strictly regulated.[9] The endocytosis of EGFR can lead to two different fates of this receptor: circulation back to the plasma membrane or degradation in lysosomes.[10] Promoting EGFR degradation could be a potential strategy for tumor treatment.

G protein pathway suppressor 2 is a small 37-kDa protein and the corresponding gene is located at 17p13.1. Also known as AMF1 (activating domain regulator 1), GPS2 is expressed in most human tissues, including the kidney.[11,12] GPS2 was originally shown to inhibit G protein-activated RAS and MAPK signaling and interfere with JNK activity in yeast and mammalian cells.[13] GPS2 was later shown to be involved in many physiological and pathological processes, including proliferation, apoptosis, DNA repair, brain development, and metabolism.[14,15] GPS2 is an epigenomic regulator involved in the regulation of inflammatory gene expression in the nucleus. In many cases, GPS2 acts as the core subunit of the basic chromatin-modified cardiac compression complex, which includes histone deacetylase 3 (HDAC3), nuclear receptor corepressor (NCOR), and retinoid and thyroid receptor (SMRT, also known as NCOR2).[16] GPS2 interacts with transcription factors and some lipid-sensing nuclear receptors.[17] In addition, studies have shown that GPS2 exerts a nontranscriptional effect in the cytoplasm; in particular, GPS2 has been associated with the regulation of tumor necrosis factor α signaling and JNK activity. GPS2 has been shown to interact with the E2 ubiquitin-binding enzyme Ubc13, which participates in K63 ubiquitination.[18] Dysregulation of GPS2 has been reported to be associated with the tumorigenesis of glioblastoma multiforme and undifferentiated spindle cell sarcoma.[19] However, the precise mechanisms by which GPS2 functions in GC have not yet been identified. In this study, the biological function and clinical significance of GPS2 in GC were examined.

2 | MATERIALS AND METHODS

2.1 | The Cancer Genome Atlas datasets

The databases applied in this study are publicly available from TCGA-STAD. All data were downloaded using TCGA assembler software, and mRNA levels were detected by RNA sequencing using V2 RSEM software.

2.2 | Patients

Two independent GC cohort TMAs were utilized in this study for IHC. The training cohort TMA was purchased from Wuhan Iwill Biological Technology Co., Ltd. Two TMAs contain a total of 230 points, including 30 pairs of cancerous and adjacent tissues, 120 cases of nonadjacent cancerous tissues, and 50 cases of unpaired adjacent cancerous tissues. The array dot diameter was 1.5 mm, and each dot represented a tissue spot from one individual specimen that was selected and pathologically confirmed. Sixteen pairs of tumor and adjacent normal gastric tissues were collected from patients at the Dongfeng General Hospital immediately after surgical resection and stored in liquid nitrogen until further use. For qPCR, 16 pairs of tissue specimens were ground in liquid nitrogen cooled mortar, and tissue powder was suspended in TRIzol reagent (Invitrogen). For western blot assay, 10 pairs of tissue specimens were ground in liquid nitrogen cooled mortar, and tissue powder was suspended in lysis buffer (50 mmol/L Tris-HCl [pH 7.4], 150 mmol/L NaCl, 1% Triton X-100, 1% sodium deoxycholate, 0.1% SDS, 1 mmol/L PMSF, and complete protease inhibitor cocktail) and cleared by centrifugation. The samples were used with the approval of the Institutional Review Board of Hubei University of Medicine and Dongfeng General Hospital affiliated to Hubei University of Medicine. All tissue samples were obtained with written informed consent from patients at the Dongfeng General Hospital.

2.3 | Cell culture

The GC lines MKN74, SGC7901, BGC823, MGC803, HGC27, and AGS and normal human gastric epithelial cell line GES1 were purchased from ATCC. SGC7901, BGC823, MGC803, HGC27, AGS, and GES1 were cultured in DMEM containing 10% FBS (HyClone Laboratories), 100 U/mL penicillin (Amresco), and 100 mg/mL streptomycin (Amresco). MKN74 cells were cultured in RPMI-1640 (HyClone Laboratories) supplemented with 10% FBS, 100 U/mL penicillin, and 100 mg/mL streptomycin. All cells were incubated in a humidified atmosphere with CO_2 at 37°C.

2.4 | Western blot analysis

Cell pellets were lysed in RIPA buffer (Merck, Millipore). Lysates were normalized for total protein (25 μg) and loaded on 8%-12% SDS polyacrylamide gel, electrophoresed, and transferred to a PVDF membrane (Millipore), followed by blocking with 5% skimmed milk at room temperature for 1 hour. The membrane was incubated with primary Abs overnight at 4°C and rinsed with TBS with Tween-20. The primary Abs used were anti-GPS2 (GeneTex), anti-EGFR, anti-phospho-EGFR (Y1045), anti-phospho-EGFR (Y1068), anti-HA, anti-Myc, anti-Flag, anti-mTOR, anti-phospho-mTOR (S2448), anti-LC3A/B (all Cell Signaling Technology), and anti-phospho-Akt (S473), anti-Akt, and anti-GAPDH (Santa Cruz Biotechnology). The blots were then washed and incubated with HRP-conjugated secondary Ab (EarthOx) at room temperature for 1.5 hours. Detection was carried out using a SuperSignal West Pico Trial kit (Pierce Biotechnology).[20]

2.5 | Real-time qPCR

Quantitative PCR was undertaken as described previously using Taq Pro Universal SYBR qPCR Master Mix (Vazyme Biotech Co., Ltd).[20] The PCR conditions consisted of the following: 95°C for 3 minutes for denaturation; 95°C for 15 seconds for annealing; and 60°C for 1 minute for extension, for 40 cycles. The threshold cycle for each sample was selected from the linear range and converted to a starting quantity by interpolation from a standard curve generated on the same plate for each set of primers (Table 1). The target gene mRNA levels were normalized for each well to the *GAPDH* mRNA levels using the $2^{-\Delta\Delta C_q}$ method.[21] Each experiment was repeated three times.

2.6 | Immunohistochemistry

Immunohistochemical analysis as well as the scoring of immunoreactivity was undertaken using the rabbit polyclonal anti-GPS2 Ab. The intensity of GPS2 staining was scored. The scores of each tumor sample were multiplied to give a final score of 0-6, and the tumors were finally determined as negative (–), score 0; lower expression (+), score 1.5 or less; moderate expression (++), score 1.5-2.5; and high expression (+++), score 2.5 or higher. Each tumor sample that scored (+) was considered negative (low expression).

TABLE 1 Primer sequences for quantitative PCR

Gene	Primer sequence
GPS2	F: AGGCGAAAGGAACAGAGTGA
	R: GAGTACCTGGGCGATTGTGT
EGFR	F: TTGCCGCAAAGTGTGTAACG
	R: GTCACCCCTAAATGCCACCG
GAPDH	F: GGTCTCCTCTGACTTCAACA
	R: GTGAGGGTCTCTCTCTTCCT

Abbreviations: F, forward; R, reverse.

2.7 | Plasmids and stable or transient transfections

GPS2 was subcloned into pLVX-HA and pcDNA3-HA vectors. Epidermal growth factor receptor was subcloned into pLVX-C-HA and pLVX-C-Myc vectors. Casitas B-lineage lymphoma was subcloned into pcDNA3-Flag-vectors. Transfection of plasmids was undertaken using Lipofectamine 3000 (Invitrogen).

To generate stable cells, lentiviral infections were used. HEK293T cells were cotransfected with viral vectors and packaging plasmids. Forty-eight hours after transfection, culture medium was supplemented with 5 μg/mL polybrene, filtered through a 0.45 μm filter, and used to infect cells of interest. Thirty-six hours after infection, cells were selected with respective antibiotics in culture medium.

2.8 | Cytotoxic assay and cell viability

Cells were seeded into a 96-well plate and precultured for 24 hours, and then transfected with plasmid or siRNA for 24 hours. Cell cytotoxicity was determined by MTT assay. Cell viability was estimated by Trypan blue dye exclusion.[22]

2.9 | Soft agar colony formation assay

Colony formation assay and soft agar colony formation analysis were carried out as described.[23]

2.10 | Invasion assay

Invasion assay was carried out as described.[24]

2.11 | Wound healing assay

Wound healing assay was carried out as described.[25]

2.12 | RNA interference

Small interfering RNA specific for GPS2 and NC siRNA was synthesized (RiboBio) and transfected using Lipofectamine 2000 (Invitrogen). The sequences were as follows: NC siRNA, 5′-UUCU CCGAACGUGUCACGUTT-3′; GPS2 siRNA #1, 5′-UAGGACUAUAAG CUGGCUG-3′, GPS2 siRNA #2, 5′-UAGAGCCAAAAGCUUCUCC-3′, and GPS2 siRNA #3, 5′-UCCAUCAUAAUGUGCCGGU-3′.

2.13 | Turnover assay

The cells were transfected with indicated plasmids. Cycloheximide was added into the media at 50 μg/mL of final concentration. The cells were harvested at the indicated time points after CHX treatment. The protein levels were analyzed by western blot. The density of protein was measured by densitometer and the integrated optical density was measured.

2.14 | Ubiquitination assay

The cells were transfected with the indicated plasmids and then treated with bortezomib (100 nmol/L; Selleck) for 24 hours and PR-619 (20 μmol/L; Selleck) for 1 hour. Then cells were lysed with lysis buffer (Roche Applied Science), 1 mmol/L DTT, 1 mmol/L PMSF, and 20 mmol/L N-ethylmaleimide and immunoprecipitated with anti-Myc Abs after 1:10 dilution with lysis buffer. The immunoprecipitates were washed three times with lysis buffer containing 0.1% SDS. Samples were then boiled before western blot analysis.

2.15 | Immunofluorescence staining

The cells were transfected with indicated plasmids. Cells were then fixed and penetrated. Primary Abs were incubated with cells at 4°C overnight. Dylight 488- or Dylight 594-conjugated secondary Abs (EarthOx) were diluted 1:500 in 3% BSA in PBS for 1.5 hours at room temperature. We used DAPI for visualization of cell nucleus. Sections were observed using an Olympus laser scanning confocal microscope with imaging software (Olympus Fluoview FV-1000).

2.16 | Autophagy assays

The cells were transfected with pQCXIP-GFP-LC3 or pmCherry-GFP-LC3 plasmid using Lipofectamine 3000 and then fixed in 4% paraformaldehyde. The percentage of cells with fluorescent dots representing GFP and mCherry translocation was counted. We used DAPI for visualization of cell nucleus. Sections were observed using an Olympus laser scanning confocal microscope with imaging software.[26]

2.17 | Acridine orange staining

The cells were transfected with indicated plasmids. Cell staining with AO (Sigma-Aldrich) was undertaken according to the protocol from the manufacturer, adding a final concentration of 5 μg/mL for a period of 10 minutes (37°C, 5% CO_2) and were examined with a confocal microscope.

2.18 | Murine models

Equal amounts of female and male nude immunodeficient mice (nu/nu), 5-6 weeks old, were purchased from Hunan SJA Laboratory Animal Co., Ltd., and maintained and monitored in a SPF environment. The mice were injected s.c. with 6×10^6 SGC7901-Vector (n = 8), AGS-Vector (n = 8) or SGC7901-GPS2^{OE} (n = 8), AGS-GPS2^{OE} cells in 100 μL DMEM into the right flank. In addition, 28 nude mice were used to detect potential tumor inhibition induced by HCQ. After being randomly divided into four groups (AGS-Vector, AGS-GPS2^{OE}, AGS-Vector + HCQ, and AGS-GPS2^{OE} + HCQ; seven mice per group), the mice were treated with either PBS or HCQ (8 mg/kg) by i.p. injection every 4 days for 6 weeks. Body weight was measured for all mice every 2 days. Caliper measurements of the longest perpendicular tumor diameters were carried out twice a week to estimate the tumor volume, using the following formula: $4\pi/3 \times (\text{width}/2)^2 \times (\text{length}/2)$. Animals were killed when tumors reached 1.5 cm or if the mice appeared moribund to prevent unnecessary morbidity. Tumor tissues were excised for western blot analysis or fixed in 10% formalin and then embedded in paraffin for H&E staining and IHC. All animal experiments were approved by the Animal Care Committee of Hubei University of Medicine (approval number 2020-021).

2.19 | Statistical analysis

All statistical analyses were carried out using GraphPad Prism 8 (GraphPad Software) and SPSS 22.0 software for Windows (IBM). Results from three independent experiments were presented as the mean ± SD unless otherwise noted. Statistically significant values were compared using Student's *t* test of unpaired data or one-way ANOVA and Bonferroni's post hoc test. *P*-values less than .05 was used to indicate a statistically significant difference.

3 | RESULTS

3.1 | Decreased mRNA expression of *GPS2* predicts poor prognosis of patients from TCGA GC cohort

To investigate the *GPS2* mRNA expression profile in human GC tissues, we first analyzed the *GPS2* expression levels in TCGA database. We found that the *GPS2* mRNA levels were significantly lower

in tumor tissues than in normal gastric tissues (Figure 1A). The expression of *GPS2* in T3+T4 GC patients was significantly lower than that in T1+T2 patients (Figure 1B). Moreover, *GPS2* was expressed at lower levels in tumors with higher degrees of lymph node metastasis (stage N1-N3) and malignancy (stage III-IV) than in tumors with lower degrees of lymph node metastasis (stage N0) and malignancy (stage I-II) (Figure 1C,D). However, there was no significant difference in the expression of *GPS2* in GC tissues with or without distant metastasis (Figure 1E). Furthermore, patients with lower *GPS2* expression showed significantly reduced survival compared to patients with higher *GPS2* expression, according to the TCGA database (Figure 1F,G). These results suggested that *GPS2* could act as a tumor suppressor in GC.

3.2 | G protein pathway suppressor 2 expressed at low levels in GC and low GPS2 expression is associated with poor prognosis

We first investigated GPS2 expression in a panel of six human GC cell lines (SGC7901, BGC823, MGC803, AGS, MKN74, and HGC27 cells) and one normal human gastric epithelial cell line (GES1 cells). Western blot analysis showed low levels of GPS2 in the AGS, SGC7901, HGC27, and BGC823 cells compared with the GES1 cells (Figure 2A). Moreover, we detected GPS2 expression in clinical human GC samples by qPCR and western blot analysis. The mRNA and protein levels of GPS2 were found to be significantly lower in 14 of 16 (87.5%) and in 8 of 10 (80.0%) of the GC tumors than in the paired normal gastric mucosa according to qPCR and western blot analysis, respectively (Figure 2B,C). We also analyzed GPS2 expression in 150 GC tissue samples and 80 adjacent cancerous tissue samples by IHC analyses of a TMA. Immunoreactivity scoring was undertaken as described.[27] We found that GPS2 was expressed at low levels in 50.67% (76 of 150) of the tumor samples, and 16.25% (13 of 80) of the adjacent cancerous tissue samples showed low GPS2 expression (Figure 2D,E). These results suggested that GPS2 might be a critical molecule for GC development. Furthermore, IHC analysis of the TMA, which included 30 paired samples from GC patients, revealed that tumor tissues showed lower staining than paired adjacent cancerous tissues (Figure 2F).

To explore the clinicopathologic significance of GPS2 in GC, all the patients were divided into a high GPS2 expression subgroup (n = 74) and a low GPS2 expression subgroup (n = 76). The relationship between GPS2 expression and clinicopathologic features is shown in Table 2. Low expression of GPS2 was positively correlated with tumor invasion depth, lymph node metastasis, and clinical stage. These results suggested that the expression of GPS2 is closely related to GC metastasis. The relative proportion of GC patients with

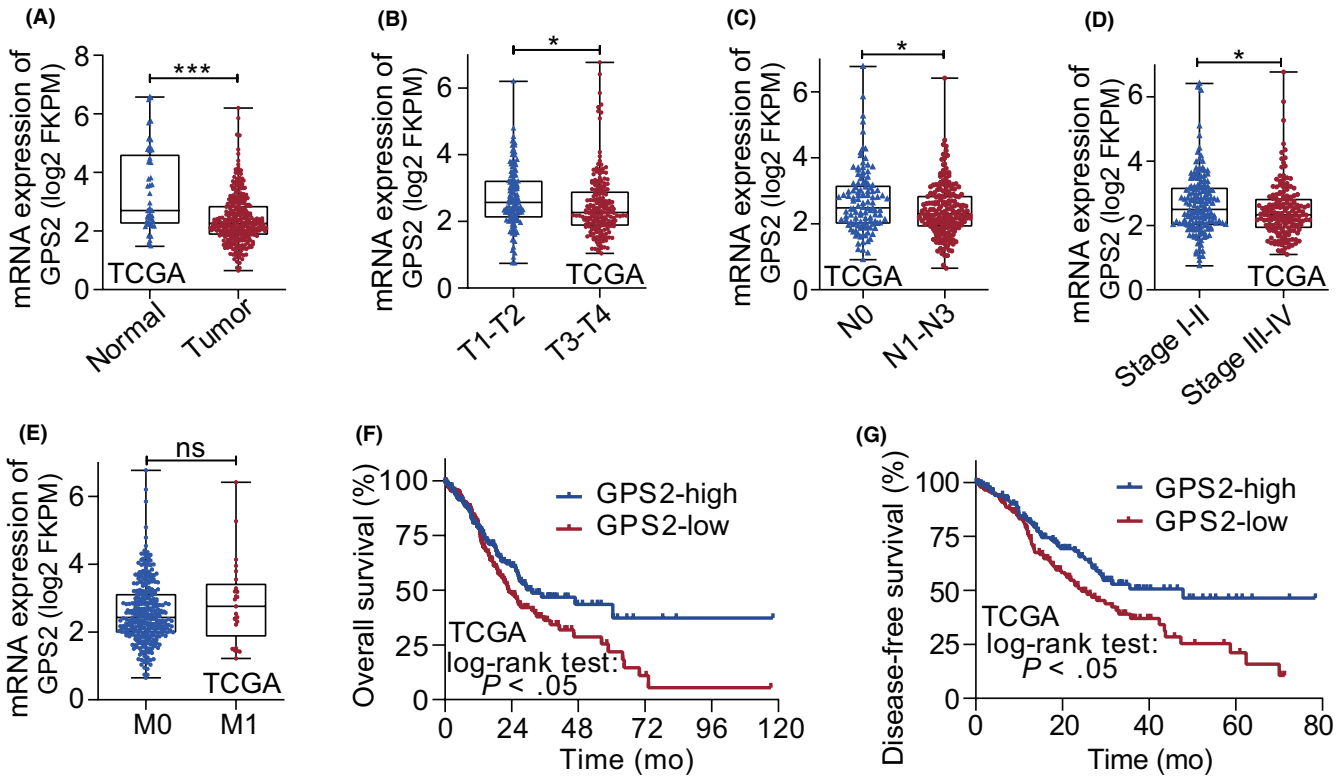

FIGURE 1 G protein pathway suppressor 2 (*GPS2*) expression in The Cancer Genome Atlas of Stomach Adenocarcinoma (TCGA-STAD) cohort. A, Differences in the expression levels of *GPS2* in normal and tumor gastric tissues. B-E, *GPS2* expression level in gastric cancer samples with different T stages (B), N stages (C), pathologic stages (D), and M stages (E). F,G, Association of *GPS2* expression in tumor tissues with overall survival and disease-free survival in TCGA-STAD was examined by Kaplan-Meier analysis. *$P < .05$; ***$P < .001$. FKPM, fragments per kilobase million

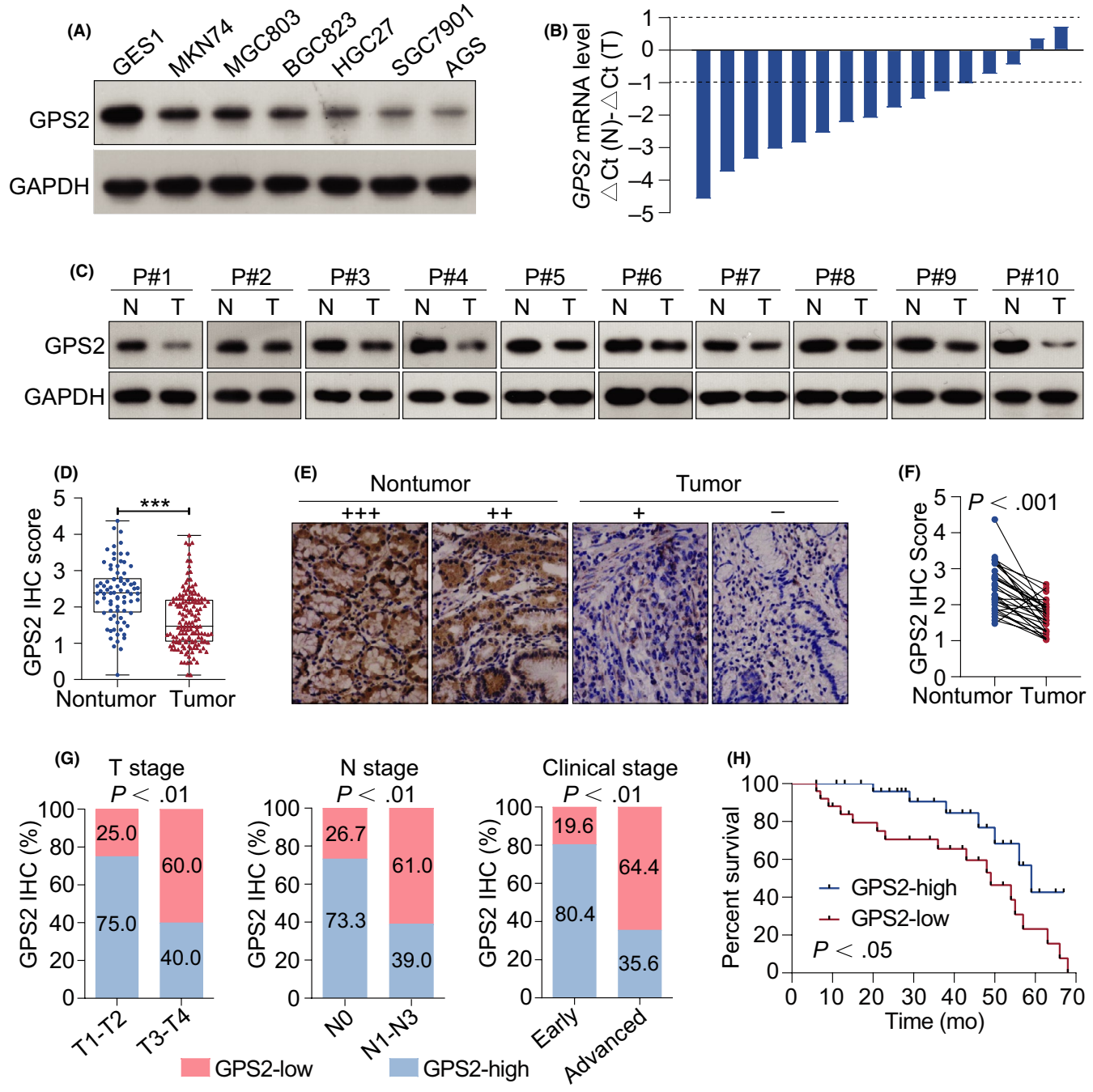

FIGURE 2 G protein pathway suppressor 2 (GPS2) is expressed at low levels in gastric cancer (GC) and low GC expression is associated with poor prognosis. A, Western blot analysis of the GPS2 protein levels in the GES1 and GC cell lines. B, Determination of the *GPS2* mRNA levels in 16 tumor tissues and paired noncancerous normal tissues from GC patients by quantitative PCR. ΔCt (N), the Ct value of *GAPDH* was subtracted from the Ct value of *GPS2* in normal gastric tissues. ΔCt (T), the Ct value of *GAPDH* was subtracted from the Ct value of *GPS2* in the cancer tissues. The bar value (ΔCt (N) – ΔCt (T)) represents the difference in the *GPS2* mRNA levels between the normal tissues and paired tumor tissues. Bar value = −1 indicates that the *GPS2* mRNA expression of the tumor tissues is 2^{-1}-fold of that of the paired normal tissues, showing that the expression of *GPS2* is decreased in the tumors. Bar value = 1 indicates that the *GPS2* mRNA expression of the tumor tissues is 2^{1}-fold of that of the paired normal tissues, showing that the expression of *GPS2* is increased in the tumors. C, Western blot analyses of GPS2 protein expression in 10 tumor tissues (T) and paired noncancerous normal tissues (N) from GC patients (P#1-P#10). D, Immunohistochemical (IHC) analysis of the GPS2 protein levels in GC tissues and normal tissues on a tissue microarray. GC tissue sections were quantitatively scored according to the percentage of positive cells and staining intensity. E, Representative images of IHC staining of GPS2 protein expression in normal tissues and two different GC tissues. F, IHC analysis of GPS2 protein levels in 30 paired GC tissues. G, Relative proportion of GC patients with low GPS2 expression in T, N, and clinical stages. H, Survival curves of GC patients with low GPS2 expression vs GC patients with high GPS2 expression. *$P < .05$; ***$P < .001$

high or low GPS2 expression in each tumor stage revealed that the number of patients with low GPS2 expression gradually increased as tumor stage progressed (Figure 2G). Survival analysis revealed that GC patients with low GPS2 expression showed poorer overall survival than those with high GPS2 expression (Figure 2H). Altogether, our present data suggested that GPS2 was expressed at low levels in GC and that a low level of GPS2 expression was a predictor of progression and poor prognosis in GC patients.

3.3 | G protein pathway suppressor 2 inhibits GC cell proliferation and invasion

Next, we explored the role of GPS2 in GC cells. SGC7901 and AGS cells were transiently transfected with a GPS2 expression plasmid (HA-GPS2) (Figure 3A). The effect of GPS2 on cell viability was investigated. The MTT assay and growth curve results showed that GPS2 overexpression reduced cell proliferation (Figure 3B,C). Colony formation assays also showed that GPS2 overexpression significantly inhibited the colony formation of SGC7901 and AGS cells (Figure 3D). To further determine the effect of GPS2 on invasion, wound healing and invasion assays were carried out. As shown in Figure 3E,F, GPS2 overexpression markedly suppressed the migration and invasion of GC cells. To confirm this result, SGC7901 and AGS cells were transfected with GPS2 siRNA, and *GPS2* mRNA expression was examined by using qPCR (Figure 3G). *GPS2* mRNA expression was markedly decreased by siRNA treatment, and GPS2 knockdown resulted in a significant increase in cell proliferation (Figure 3H) and colony formation (Figure 3I). Furthermore, the invasion assay showed that GPS2 knockdown markedly promoted the invasion of GC cells (Figure 3J). Taken together, these data suggested that GPS2 inhibited GC cell proliferation and invasion.

3.4 | G protein pathway suppressor 2 downregulates EGFR protein expression level and inhibits its downstream signaling pathway

We discovered that, in GC cell lines transiently overexpressing GPS2, the protein expression level of EGFR, a key signaling molecule for cell growth,[28] was significantly downregulated (Figure 4A). We next evaluated whether GPS2 affected *EGFR* transcription level by qPCR. The results suggested that GPS2 had no significant effect on *EGFR* mRNA expression (Figure 4B). To further confirm the effect of GPS2 on EGFR protein level in GC cells, siRNA was used to knock down GPS2 in SGC7901 and AGS cells. Knockdown of GPS2

TABLE 2 Characteristics of G protein pathway suppressor 2 (GPS2) expression in gastric cancer patients

	GPS2 expression			
	All (n = 150)	Low (n = 76)	High (n = 74)	
Characteristic	No.	No.	No.	*P* value[a]
Age (years)				
<60	106	55	51	>.05
≥60	44	21	23	
Gender				
Male	107	53	54	>.05
Female	43	23	20	
Clinical stage				
Early (IA-IIB)	46	9	37	<.01
Advanced (IIIA-IV)	104	67	37	
Pathologic grade				
I-II	25	15	10	>.05
III-IV	125	61	64	
Invasive depth				
T1-T2	40	10	30	<.01
T3-T4	110	66	44	
Lymph node stage				
N0	45	12	33	<.01
N1-N3	105	64	41	
Tumor size (cm)				
<7	122	64	58	>.05
≥7	28	12	16	

[a]χ^2 test.

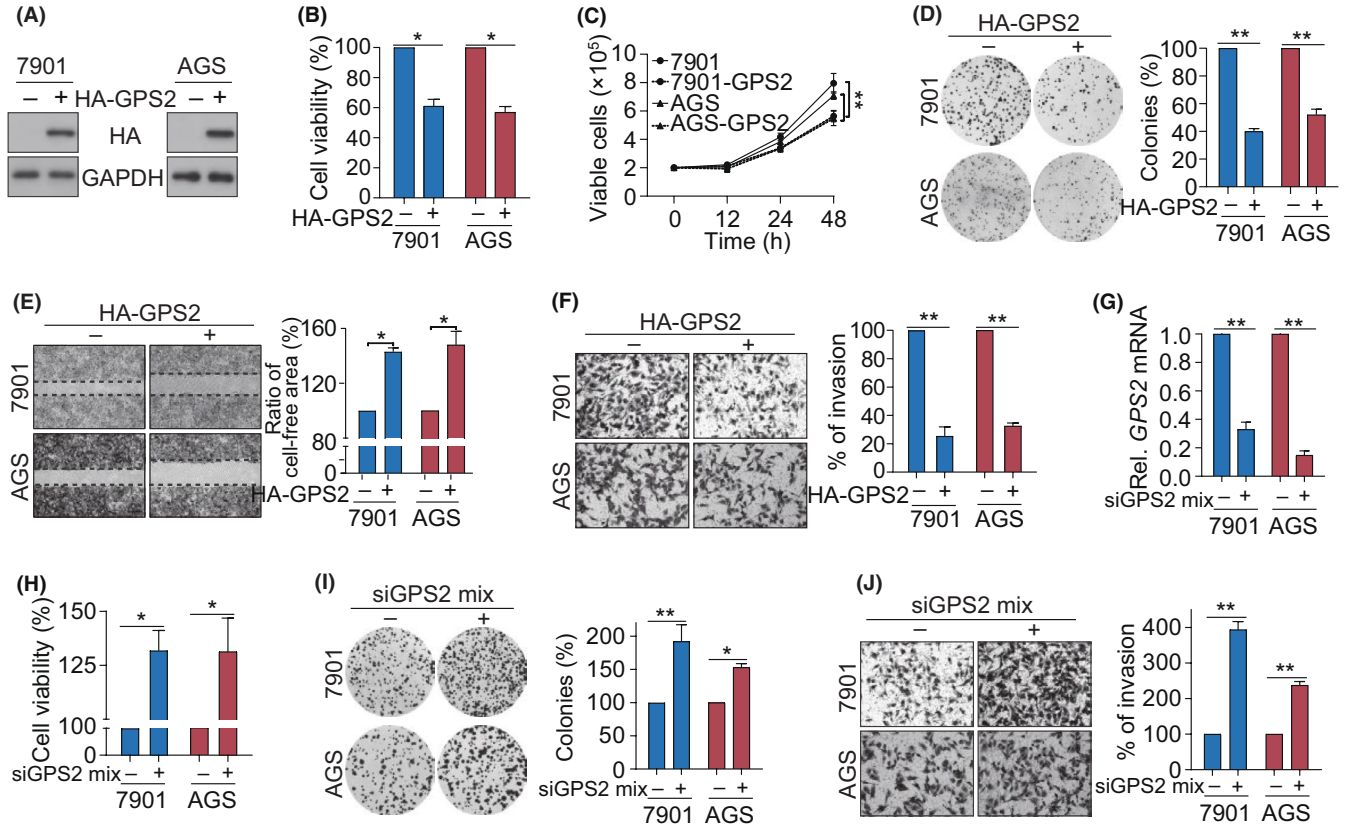

FIGURE 3 G protein pathway suppressor 2 (GPS2) inhibits gastric cancer cell proliferation and invasion. A, SGC7901 and AGS cells were transfected with the indicated vectors, and GPS2 expression was analyzed by western blot. B,C, SGC7901 and AGS cells were transfected with the indicated vectors for 48 h, and cell viability was evaluated by MTT and cell counting assays. D, SGC7901 and AGS cells were stably transfected with HA-GPS2 or vector alone. Colony formation was evaluated by clone formation assay. E, The migration of SGC7901 and AGS cells stably overexpressing GPS2 was monitored with a wound healing assay. F, Invasion of SGC7901 and AGS cells stably overexpressing GPS2 was monitored with a Transwell invasion assay. G, SGC7901 and AGS cells were transfected with GPS2 siRNA for 48 h; *GPS2* expression was analyzed by quantitative PCR. H, SGC7901 and AGS cells were transfected with GPS2 siRNA for 48 h; cell viability was evaluated by MTT assay. I, SGC7901 and AGS cells were transfected with GPS2 siRNA for 48 h; colony formation was evaluated by clone formation assay. J, SGC7901 and AGS cells were transfected with GPS2 siRNA for 48 h; invasion was evaluated by Transwell invasion assay. $^{*}P < .05$; $^{**}P < .01$

markedly increased the EGFR protein levels (Figure 4C). However, the *EGFR* mRNA levels were not notably different (Figure 4D). These data suggested that GPS2 negatively regulated the EGFR levels at the posttranscriptional level. We next examined whether GPS2 expression affected EGFR-mediated downstream signaling pathways. We constructed SGC7901 and AGS cell lines stably overexpressing GPS2. Western blot analysis suggested that the phosphorylation of AKT and mTOR was significantly decreased in GPS2-overexpressing cells (Figure 4E,F). We also detected the ERK and STAT3 signals downstream of EGFR, and the results showed that the overexpression of GPS2 did not affect ERK and STAT3 through EGFR (Figure S1). In addition, knockdown of GPS2 markedly increased the levels of phosphorylated AKT and mTOR (Figure 4G,H). The above data indicated that GPS2 reduced EGFR protein levels and modulated EGFR/AKT/mTOR signaling.

Erlotinib is a small-molecule inhibitor of EGFR tyrosine kinase that reduces the growth and metastasis of cancer cells.[29] To examine whether the effects of GPS2 on the growth and invasion of GC cells were dependent on EGFR, we treated SGC7901 and AGS cells with GPS2 siRNA and erlotinib. The MTT assays showed that erlotinib clearly reduced the effect of GPS2 knockdown on promoting cell proliferation (Figure 4I). The invasion assays suggested that erlotinib markedly decreased the effect of GPS2 knockdown on enhancing cell invasion (Figure 4J).

3.5 | G protein pathway suppressor 2 reduces EGFR protein stability through c-Cbl-mediated ubiquitination and then lysosomal degradation

Next, we blocked protein synthesis with the protein synthesis inhibitor CHX and found that GPS2 overexpression decreased the rate of EGFR turnover in the presence of CHX (Figure 5A), and GPS2 knockdown enhanced the rate of EGFR turnover in the presence of CHX (Figure S2), suggesting that GPS2 reduced EGFR protein stability.

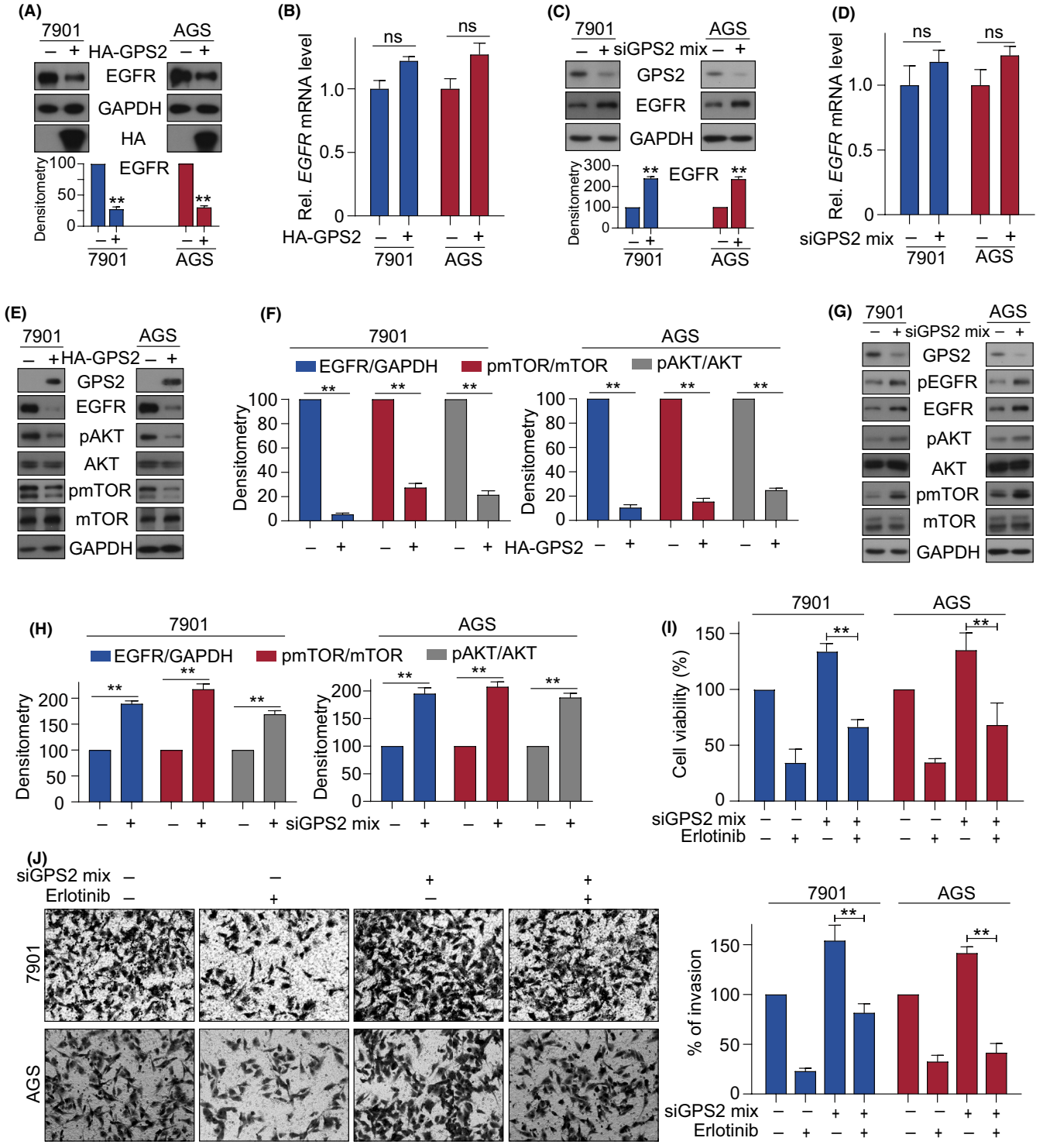

FIGURE 4 G protein pathway suppressor 2 (GPS2) downregulates the protein expression of epidermal growth factor receptor (EGFR) and inhibits its downstream signaling pathways. A, SGC7901 and AGS cells were transfected with the indicated vectors for 48 h, and protein expression was analyzed by western blot. B, SGC7901 and AGS cells were transfected with the indicated vectors for 48 h, and *EGFR* expression was analyzed by quantitative PCR (qPCR). C, SGC7901 and AGS cells were transfected with GPS2 siRNA for 48 h, and protein expression was analyzed by western blot. D, SGC7901 and AGS cells were transfected with GPS2 siRNA for 48 h, and *EGFR* expression was analyzed by qPCR. E,F, SGC7901 and AGS cells were stably transfected with HA-GPS2 or vector alone. Western blot was carried out using the indicated Abs. G,H, SGC7901 and AGS cells were transfected with GPS2 siRNA for 48 h, and protein expression was analyzed by western blot. I, SGC7901 and AGS cells were transfected with GPS2 siRNA for 48 h and then treated with erlotinib (60 μmol/L) for 24 h. Cell viability was evaluated by MTT assay. J, SGC7901 and AGS cells were transfected with GPS2 siRNA for 48 h and then treated with erlotinib (60 μmol/L) for 24 h. Invasion was evaluated by Transwell invasion assay. $^{**}P < .01$. ns, not significant

The ubiquitin–proteasomal pathway and lysosomal pathway are the two main degradation pathways in cells.[30] We further used inhibitors of these two degradation pathways to elucidate the pathway by which GPS2 mediated EGFR degradation. The results suggested that the proteasome inhibitors (MG132 and bortezomib) did not prevent the GPS2 overexpression-induced degradation of EGFR (Figure 5B). However, the lysosomal protease inhibitor HCQ significantly suppressed the GPS2 overexpression-induced degradation of EGFR (Figure 5C), suggesting that GPS2-induced EGFR degradation occurred through lysosomes. Immunofluorescence analysis showed increased colocalization of EGFR with the early endosome marker EEA1 and the late endosome and lysosome marker LAMP-1 in GPS2-overexpressing cells (Figure 5D,E), suggesting that GPS2 promoted the trafficking of EGFR to lysosomes. It has been well shown that the binding of EGF stimulates the rapid internalization of EGFR by stimulating c-Cbl (henceforth: Cbl) E3-ligase activity.[31] Phosphorylated EGFR creates a docking site for Cbl, transports it from the cytoplasm to the plasma membrane, and ubiquitinates EGFR.[32] We then measured the endogenous EGFR protein levels in GC cells transfected with HA-GPS2 after different durations of EGF stimulation. The results indicated that GPS2 clearly enhanced the EGF-induced internalization of EGFR (Figure 5F,G). These data suggested that GPS2 accelerated EGF-stimulated EGFR degradation. To further investigate the impact of GPS2 on EGFR stability, we assessed the ubiquitination of EGFR and found that GPS2 overexpression increased the levels of ubiquitinated EGFR (Figure 5H). The ubiquitination of EGFR depends on the binding of EGFR and Cbl.[9] We wanted to determine whether GPS2 affects the binding of EGFR and Cbl. Through immunoprecipitation experiments, we found that GPS2 promoted the binding of EGFR and Cbl (Figure 5I). It has been reported that Cbl interacts with EGFR either directly through phosphorylated Y1045, or indirectly through Grb2, which binds to phosphorylated Y1068 or Y1086.[31] Then we investigated the GPS2-overexpressing cells and found that the phosphorylation of Y1045 (pY1045) in EGFR were elevated, whereas the levels of Cbl and pY1068 and pY1086 had no significant changes (Figure 5J), suggesting that GPS2 increased the direct binding between Cbl and EGFR at pY1045. Taken together, these results suggested that GPS2 reduced EGFR protein stability through Cbl-mediated ubiquitination and lysosomal degradation.

3.6 | G protein pathway suppressor 2 activates autophagy and promotes autophagic flux by destabilizing EGFR

Emerging evidence indicates that the EGFR-mediated signaling pathway plays a critical role in the induction of autophagy in various cancers and that targeting EGFR-mediated autophagy is a potential strategy for cancer treatment.[33] We next sought to investigate whether GPS2 overexpression could increase the rate of autophagy. The formation of autophagosomes is accompanied by a marked redistribution of LC3 from the cytosol to autophagosomes. Figure 6A shows that overexpression of GPS2 increased the levels of the lipidated form of LC3 (LC3-II). In addition, confocal microscopy revealed increased LC3 puncta formation in GPS2-overexpressing SGC7901 and AGS cells, while diffuse, cytoplasmic green fluorescence was observed in vector control SGC7901 and AGS cells (Figure 6B). Moreover, we found that HCQ significantly suppressed the autophagic flux induced by GPS2 overexpression (Figure 6C,D), suggesting that GPS2-induced autophagy is late autophagy mediated by lysosomes. The inside of the lysosome is an acidic environment. We then used AO staining to detect the pH of the lysosomes. We observed that the autolysosomes in GPS2-overexpressing cells were acidic (Figure 6E). Finally, tandem mCherry-GFP-LC3 reporter assays were used to assess the autophagic flux. SGC7901 and AGS cells stably overexpressing GPS2 were transfected with the mCherry-GFP-LC3 plasmid, and the distribution of the mCherry-GFP-LC3 fusion protein was analyzed. The GPS2-overexpressing cells showed an increase in red-yellow punctate fluorescence (Figure 6F,G), indicating that GPS2 overexpression increased the fusion of autophagosomes and lysosomes to promote the autophagic flux. Furthermore, we restored the expression of EGFR in GPS2-overexpressing cells and determined the effect of EGFR on GPS2-induced autophagy. As we hypothesized, the overexpression of EGFR in GPS2-overexpressing GC

FIGURE 5 G protein pathway suppressor 2 (GPS2) reduces epidermal growth factor receptor (EGFR) protein stability through Casitas B-lineage lymphoma (Cbl)-mediated ubiquitination and lysosomal degradation. A, SGC7901 and AGS cells were transfected with the indicated plasmids and then treated with cycloheximide (CHX; 50 μg/mL) for the indicated times. B, SGC7901 and AGS cells were stably transfected with HA-GPS2 or vector alone. Stably transfected SGC7901 and AGS cells were treated with bortezomib (100 nmol/L) or MG132 (2 μmol/L) for 24 h. Western blot analysis was carried out using the indicated Abs. C, SGC7901 and AGS cells were stably transfected with HA-GPS2 or vector alone. Stably transfected SGC7901 and AGS cells were treated with hydroxychloroquine (HCQ; 10 μmol/L) for 24 h. Western blot analysis was carried out using the indicated Abs. D, SGC7901 and AGS cells stably transfected with HA-GPS2 and control plasmid were stained with anti-EGFR (green) and anti-early endosome antigen 1 (EEA1) (red) and analyzed by immunofluorescence assay. Scale bar = 15 μm. E, SGC7901 and AGS cells stably transfected with HA-GPS2 and control plasmid were stained with anti-EGFR (green) and anti-lysosomal associated membrane protein 1 (LAMP-1; red) and analyzed by immunofluorescence assay. Scale bar = 15 μm. F,G, SGC7901 and AGS cells were transfected with the indicated plasmids and then treated with epidermal growth factor (EGF; 100 μg/mL) for the indicated times. H, SGC7901 and AGS cells were transfected with the Myc-EGFR, HA-Ub, and/or HA-GPS2 plasmids for 48 h. Western blot analysis was carried out using the indicated Abs. I, HEK293T cells were transfected with Flag-Cbl, Myc-EGFR, and/or HA-GPS2 plasmids for 48 h, and lysates were immunoprecipitated as indicated. J, SGC7901 and AGS cells were stably transfected with HA-GPS2 or vector alone. Western blot analysis was carried out using the indicated Abs. $^{*}P < .05$; $^{**}P < .01$

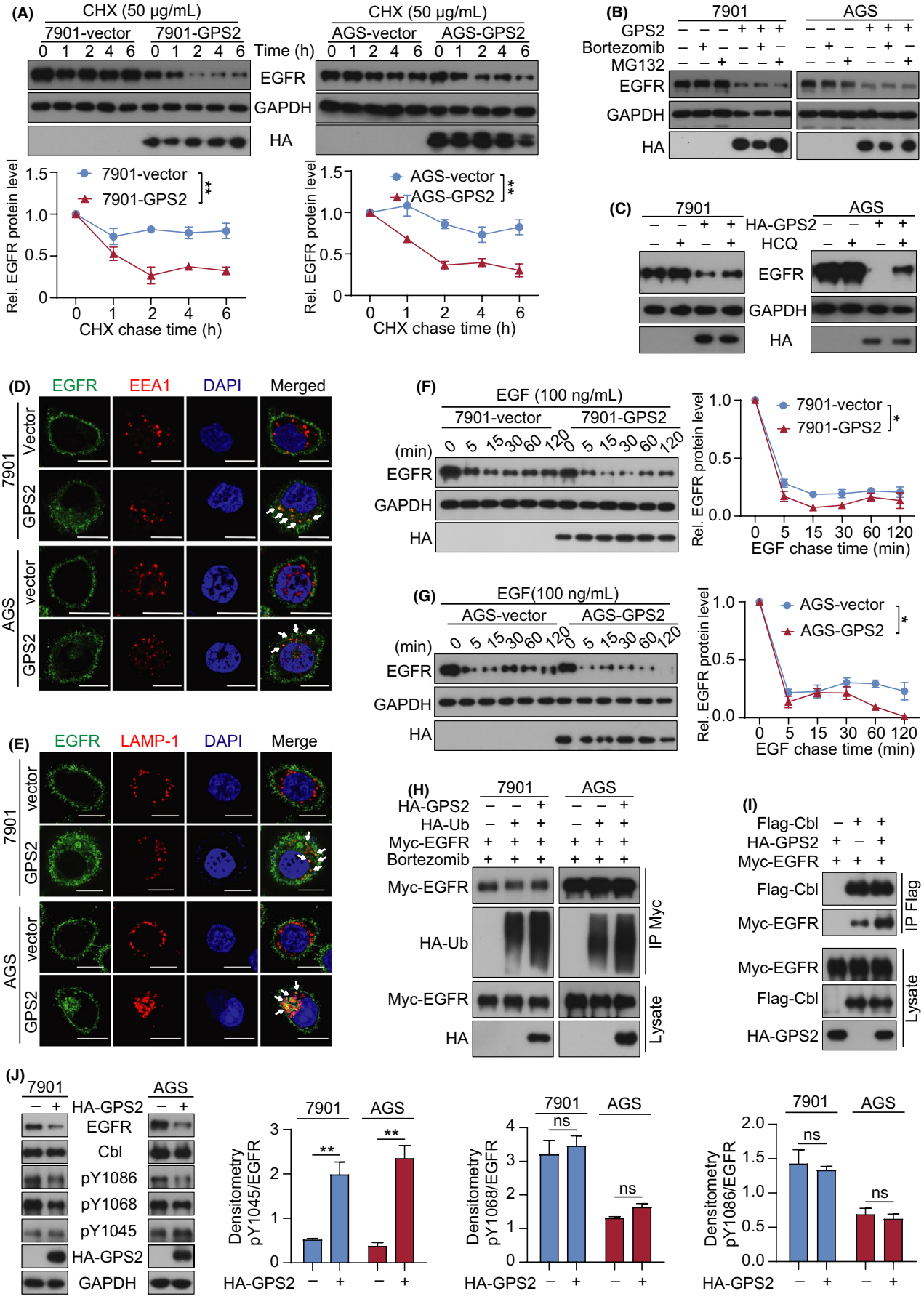
(A)
CHX (50 μg/mL)
7901-vector
7901-GPS2
AGS-vector
AGS-GPS2
Time (h)
EGFR
GAPDH
HA
Rel. EGFR protein level
CHX chase time (h)
(B)
7901
AGS
GPS2
Bortezomib
MG132
(C)
HA-GPS2
HCQ
(D)
EGFR
EEA1
DAPI
Merged
Vector
(E)
LAMP-1
Merge
(F)
EGF (100 ng/mL)
(min)
EGF chase time (min)
(G)
(H)
HA-Ub
Myc-EGFR
IP Myc
Lysate
(I)
Flag-Cbl
IP Flag
(J)
Cbl
pY1086
pY1068
pY1045
Densitometry pY1045/EGFR
Densitometry pY1068/EGFR
Densitometry pY1086/EGFR
ns

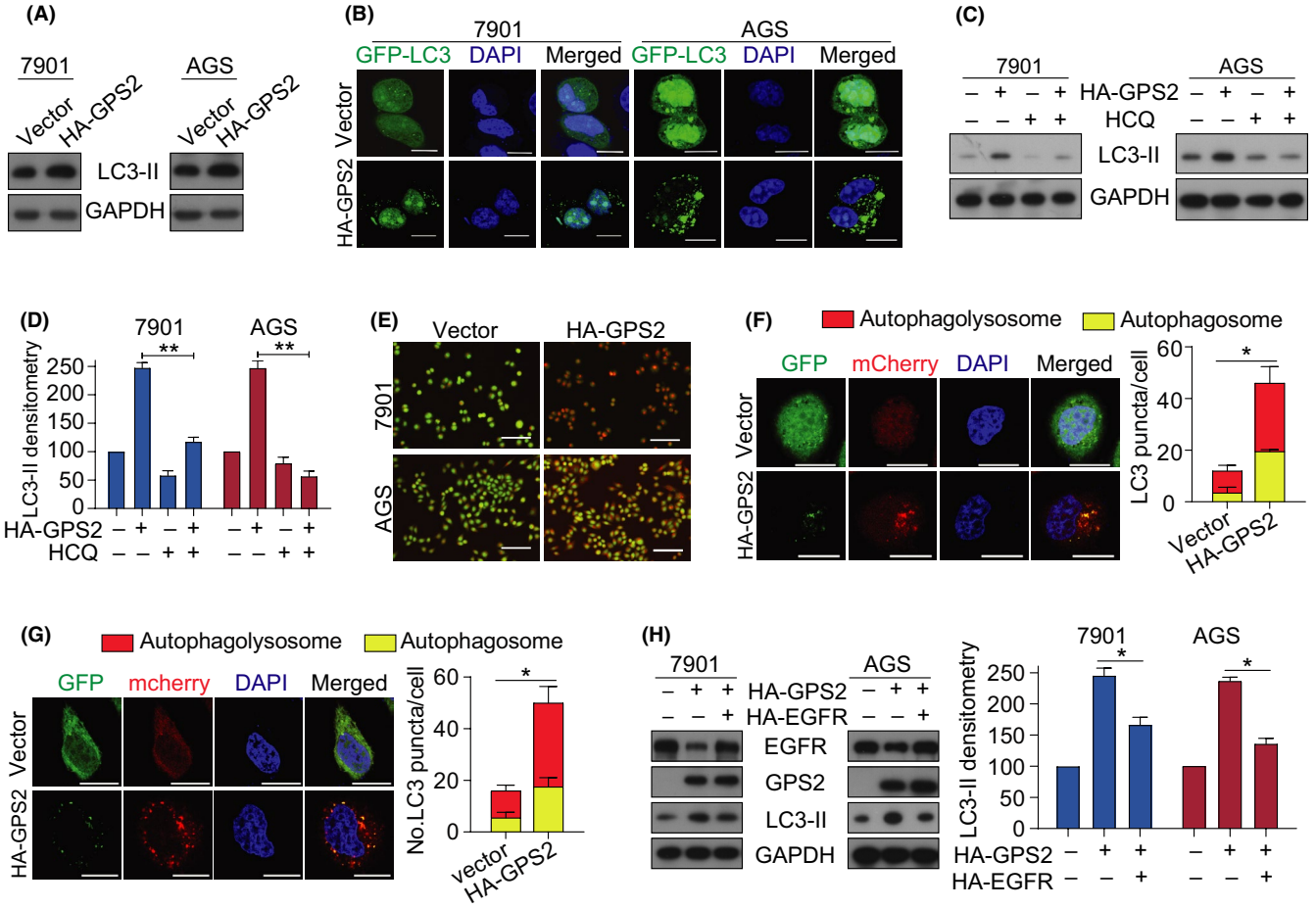

FIGURE 6 G protein pathway suppressor 2 (GPS2) activates autophagy and promotes autophagic flux. SGC7901 and AGS cells were stably transfected with HA-GPS2 or vector alone. A, Western blot analysis was carried out using the indicated Abs. B, Stably transfected SGC7901 and AGS cells were transfected with the pQCXIP-GFP-LC3 plasmid for 24 h and assessed by immunofluorescence analyses. Scale bar = 15 μm. C,D, Stably transfected SGC7901 and AGS cells were treated with hydroxychloroquine (HCQ; 10 μmol/L) for 24 h. Western blot analysis was carried out using the indicated Abs. E, SGC7901 and AGS cells were stably transfected and subjected to acridine orange staining. Scale bar = 100 μm. F,G, Stably transfected SGC7901 and AGS cells were transfected with mCherry-GFP-LC3 plasmid for 24 h and assessed by immunofluorescence analyses. Scale bar = 15 μm. H, Stably transfected SGC7901 and AGS cells were transfected with the HA-EGFR plasmid for 48 h. Western blot analysis was carried out using the indicated Abs. *$P < .05$; **$P < .01$. LC3-II, lipidated form of microtubule-associated protein 1 light chain 3

cells could significantly inhibit the expression of LC3-II, suggesting that GPS2 activated autophagy, at least in part, by destabilizing EGFR.

3.7 | G protein pathway suppressor 2 suppresses the growth xenograft GC tumors in vivo

To investigate the function of GPS2 in vivo, two xenograft tumor models were established by using SGC7901 and AGS cells stably transfected with HA-GPS2 or vector alone. Stable GPS2^{OE} and vector control SGC7901 and AGS cells were s.c. injected into nude mice, and tumor growth was monitored (Figure 7A). The xenograft tumor burdens were significantly decreased in the mice s.c. injected with SGC7901 or AGS cells stably overexpressing GPS2 compared to those in the mice s.c. injected with SGC7901 or AGS cells transfected with the vector alone (Figure 7B-F). We also monitored the weight of the nude mice (Figure 7G,H). All of the mice were killed, and the tumor specimens were examined by western blot analysis and IHC. The results showed that the expression levels of EGFR and Ki67 were downregulated and the expression level of LC-3II was upregulated in the GPS2^{OE} group (Figure 7I-K). In addition, to assess the role of EGFR in GPS2 tumor suppression, we gave HCQ, a lysosomal inhibitor, to GPS2^{OE} xenografted nude mice. The results show that for the vector group, HCQ had a certain anticancer effect. For the GPS2^{OE} group, HCQ antagonized the tumor suppressor effect of GPS2 (Figure 7L-N), which indicated that EGFR is at least partially involved in the tumor suppressor effect of GPS2 in vivo.

Overall, we conclude that GPS2 inhibited GC growth and invasion and induced cancer cell autophagy mainly through destabilizing EGFR (Figure 8).

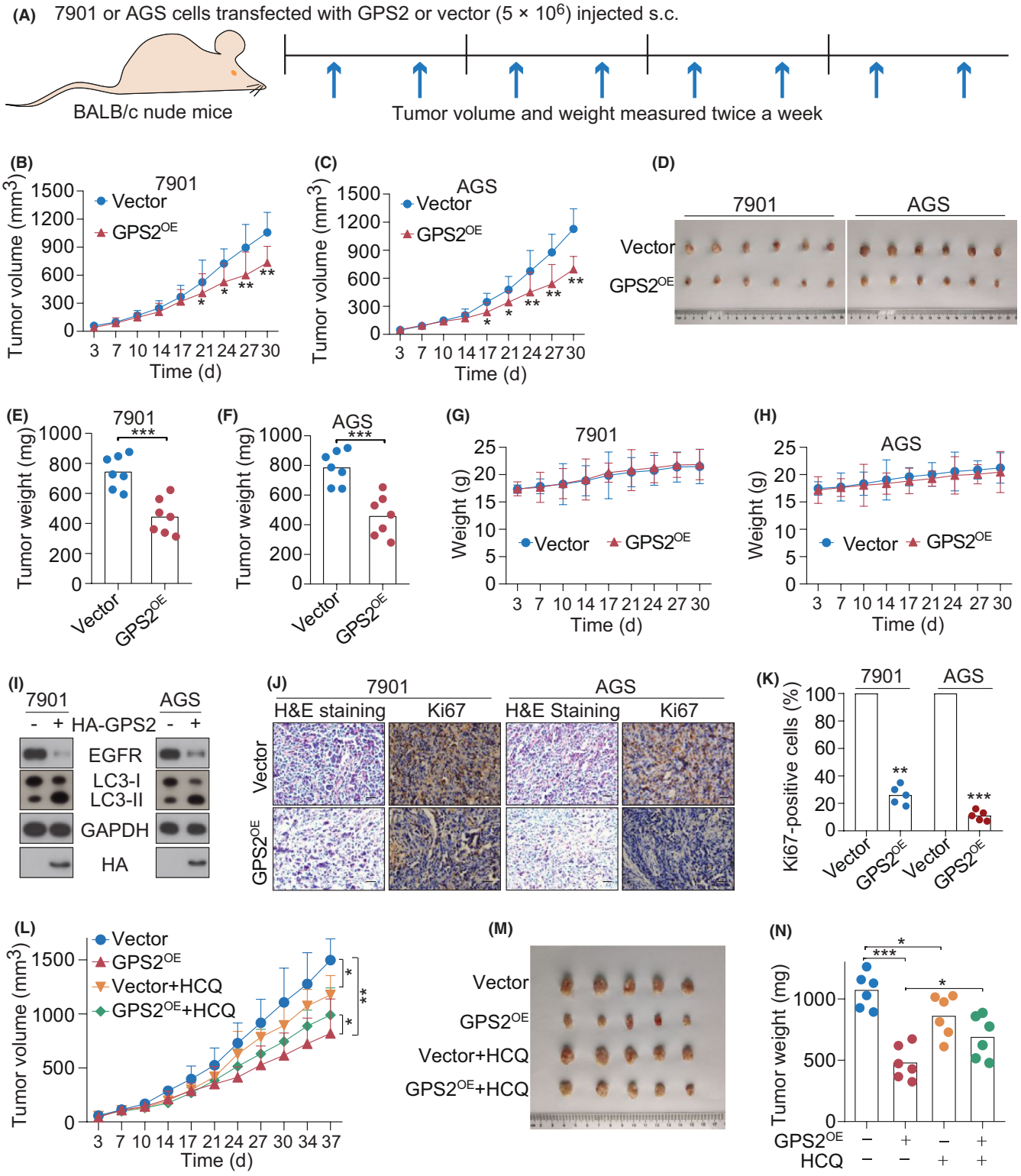

FIGURE 7 G protein pathway suppressor 2 (GPS2) suppresses gastric cancer tumorigenesis in vivo. A, Experimental design of the establishment of xenograft tumor models. B,C, Tumor volumes were calculated twice a week starting on the day mice were injected with stable GPS2^{OE} or vector cells. D, Images of xenograft tumors obtained from differentially treated mice after 4 weeks. E,F, Weights of tumors from each group at the end of the study. G,H, Murine body weight was calculated twice a week starting on the day mice were injected with stable GPS2^{OE} or vector cells. I, Expression levels of indicated proteins in xenograft tumors were analyzed by western blot. J,K, Representative tumor tissues were sectioned and subjected to H&E staining and immunohistochemical staining for Ki67. L, Murine models were treated with PBS or 8 mg/kg hydroxychloroquine (HCQ) and tumor volumes were calculated twice a week. M, Images of xenograft tumors excised from each group of mice at the end of the study. N, Weight of tumors excised from each group of mice at the end of the study. Scale bar = 100 μm. *$P < .05$; **$P < .01$, ***$P < .001$

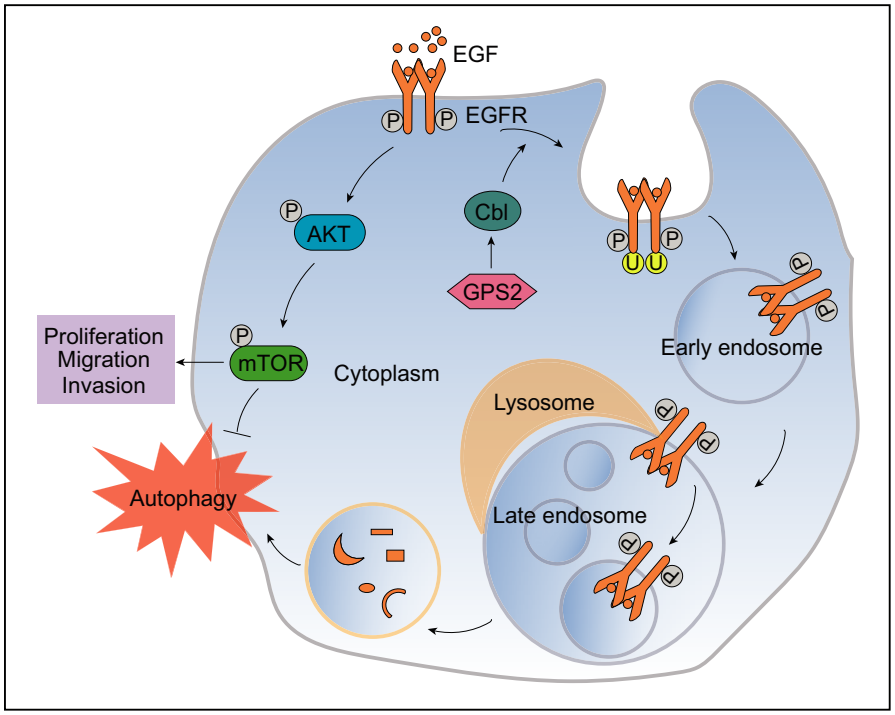

FIGURE 8 Proposed model illustrating how G protein pathway suppressor 2 (GPS2) suppresses gastric cancer by destabilizing epidermal growth factor receptor (EGFR). GPS2 promotes Casitas B-lineage lymphoma (Cbl)-dependent EGFR ubiquitylation, and then non-clathrin-mediated internalization, followed by endosome delivery to lysosomal degradation. The AKT/mTOR signal downstream of EGFR is inhibited in this process, which in turn activates autophagy, and inhibits cell proliferation and invasion. EGF, epidermal growth factor

4 | DISCUSSION

Metastatic GC is still a challenging disease with no effective clinical treatment. Therefore, it is urgent to identify early diagnostic markers and to discover new potential treatment targets.

As a critical subunit of the NCOR/SMRT complex, GPS2 is mainly located in the nucleus.[17] Recent studies have shown that GPS2 plays important roles in the cytoplasm, including promoting erythroid differentiation by controlling the stability of the EKLF protein[34] and regulating multiple stages of B cell development by inhibiting Ubc13-mediated ubiquitination.[35] However, few studies have explored the relationship between the expression of GPS2 and the progression and prognosis of cancer. Here, we sought to explore other possible mechanisms by which GPS2 functions in the cytoplasm to provide additional approaches for inhibiting tumorigenesis. In the TCGA-STAD cohort, GC cell lines, and patient tumor tissues, we showed that the expression of GPS2 was significantly reduced (Figures 1 and 2). Low expression of GPS2 was related to pathological grade and lymph node stage but might not be significantly correlated with distant metastasis (Figure 2, Table 2). These findings showed that GPS2 could be involved in the progression of GC and be a significant prognostic biomarker for GC patients. The clinical data described above prompted us to carry out a series of in vitro and in vivo experiments to explore the possible underlying mechanisms.

Next, a series of in vitro and in vivo experiments established GPS2 as a tumor suppressor in GC. Overexpression of GPS2 in GC cells inhibited cell growth, clone formation in vitro, and tumorigenicity in mice bearing xenografts. Xenograft tumors overexpressing GPS2 showed a slower growth rate and decreased Ki67 expression (Figure 7). Migration and invasion are important characteristics of cancer cell metastasis.[25] Here, we showed that GPS2 in GC cells suppressed cell migration and invasion in vitro. In contrast, downregulation of GPS2 expression promoted the growth, colony formation, migration, and invasion of GC cells (Figure 3). G protein pathway inhibitor 2 has recently been shown to be a tumor suppressor in two other cancer types, liposarcoma,[36] and breast cancer.[37] In liposarcoma, GPS2 knockdown enhanced proliferation, migration, and cell cycle progression of SW872 cell line.[36] In breast cancer, loss of GPS2 expression led to increased proliferation and migration of the MDA-MB-231 cell line through constitutive AKT activation.[37] Hence, GPS2 is likely to be an important tumor suppressor that inhibits the progression of several types of tumors.

Epidermal growth factor receptor controls a variety of biological processes in tumor cells, including cell proliferation, invasion, apoptosis, and drug resistance.[28] In addition, EGFR plays a vital role in physiological and pathological processes.[38] Therefore, it is important to investigate the stability of EGFR in tumor cells. In this study, we revealed that GPS2 downregulated the protein expression level of EGFR and inhibited its downstream AKT/mTOR signaling. We further confirmed that GPS2 suppressed GC cell proliferation and metastasis through EGFR-mediated signaling pathways using erlotinib (Figure 4). Epidermal growth factor receptor is a main factor upstream of the AKT/mTOR pathway.[39] Epidermal growth factor receptor, as a new downstream molecule of GPS2, could explain why the loss of GPS2 expression enhanced proliferation and migration in liposarcoma SW872 cells and breast cancer MDA-MB-231 cells, as described above. Non-clathrin-mediated endocytosis plays a major role in the regulation of EGFR fate by targeting it to lysosomes for degradation.[9] Wang et al also reported that EGFR is degraded through the proteasome pathway.[40] We used

a protein synthesis inhibitor (CHX), proteasome inhibitors (bortezomib and MG132), and a lysosomal inhibitor (HCQ) and detected the expression of EGFR in GC cells stably overexpressing GPS2; we ultimately found that GPS2 overexpression promotes the protein instability of EGFR through the lysosome pathway (Figure 5A-C). Both the CME and NCE internalization pathways lead to the same early endosomal compartment.[41] Next, immunofluorescence experiments proved that EGFR colocalized with the early endosomal marker EEA1 and lysosomal marker LAMP-1 (Figure 5D,E), indicating that GPS2 promotes the degradation of EGFR through the NCE pathway. Non-clathrin-mediated is reported to have potential tumor suppressor properties.[42] Here, we proved that GPS2's downregulation of EGFR through the NCE pathway also indicated the tumor suppressor effect of GPS2. Physiologically high doses of EGF often activate the NCE of EGFR.[43] Furthermore, we proved that high expression of GPS2 enhanced the NCE of EGFR at high concentrations of EGF (Figure 5F,G). Non-clathrin-mediated of EGFR has been shown to be mediated by ubiquitination, and this ubiquitination is specifically regulated by the activity of the E3 ligase Cbl.[9] Therefore, Cbl is a key molecule that negatively regulates EGFR. The high expression of GPS2 enhanced the binding of Cbl to EGFR and further increased its ubiquitination (Figure 5H,I). As mentioned above, the ubiquitination regulation of EGFR by Cbl is either directly, through binding to its pY1045 site, or indirectly, through Grb2 binding to the pY1068 or pY1086 site.[31] Our experiment ruled out the possibility of Cbl indirectly binding to EGFR through Grb2 (Figure 5J). The direct binding of Cbl to pY1045 could be more stable, thereby more effectively leading to the increase and degradation of EGFR ubiquitination.

Previously, EGFR was reported to regulate autophagy through several downstream signaling pathways.[33,44] We observed markedly increased autophagy and enhanced autophagic flux in GPS2-overexpressing GC cells (Figure 6A-G), suggesting that the low expression of EGFR caused by GPS2 could be the main driver of autophagy. Furthermore, restoring EGFR expression in cells overexpressing GPS2 inhibited autophagy (Figure 6H). This showed that GPS2 induced autophagy by destabilizing EGFR in GC cells. Both endocytosis and autophagy transport cellular cargo to the lysosome for degradation. Recent research has started to reveal the mechanism by which endocytic and autophagy compartments can work together to promote their optimal activity. Autophagosomes need to fuse with late endosomes, not directly with lysosomes; this mixing chamber then fuses with lysosomes and promotes the degradation of the contents.[4] Fraser et al reported that the ablation of autophagy-essential players disrupts EGF-induced endocytic trafficking of EGFR.[45] This indicated that autophagy might also be involved in the endocytosis of EGFR induced by GPS2; however, follow-up experiments are required.

In conclusion, low expression of GPS2 is a common event in GC, and low expression of GPS2 serves as a biomarker of reduced overall survival and poor prognosis. Moreover, GPS2 overexpression destabilizes EGFR, thereby reducing cell proliferation and invasion and promoting autophagy. Our results confirmed that GPS2 serves as a new tumor suppressor in GC and could be a novel therapeutic target in GC.

ACKNOWLEDGMENTS

This work was supported by grants from the National Natural Science Foundation of China (nos. 82072928 and 81802387), the Foundation for Innovative Research Group of Hubei Provincial Department of Science and Technology (no. 2021CFA071), the Foundation for Innovative Research Team of Hubei Provincial Department of Education (no. T201915), the Grants of Open Ended Design Project from Hubei Key Laboratory of Embryonic Stem Cell Research (no. 2020ESOF007), the Principal Investigator Grant of Hubei University of Medicine (no. HBMUPI201806), the Faculty Development Grants from Hubei University of Medicine (no. 2018QDJZR03), the Scientific and Technological Project of Shiyan City of Hubei Province (nos. 21Y08 and 21Y09), and the National Training Program of Innovation and Entrepreneurship for Undergraduates (no. 202110929002).

CONFLICT OF INTEREST

The authors declare no conflicts of interest for this article.

ORCID

Ying Liu https://orcid.org/0000-0001-7423-5169

REFERENCES

1. Sung H, Ferlay J, Siegel RL, et al. Global cancer statistics 2020: GLOBOCAN estimates of incidence and mortality worldwide for 36 cancers in 185 countries. *CA Cancer J Clin*. 2021;71:209-249.
2. Chen W, Zheng R, Baade PD, et al. Cancer statistics in China, 2015. *CA Cancer J Clin*. 2016;66:115-132.
3. Jemal A, Tiwari RC, Murray T, et al. Cancer statistics, 2004. *CA Cancer J Clin*. 2004;54:8-29.
4. Murrow L, Debnath J. ATG12-ATG3 connects basal autophagy and late endosome function. *Autophagy*. 2015;11:961-962.
5. Weddell JC, Imoukhuede PI. Integrative meta-modeling identifies endocytic vesicles, late endosome and the nucleus as the cellular compartments primarily directing RTK signaling. *Integrat Biol*. 2017;9:464-484.
6. Molaei F, Forghanifard MM, Fahim Y, Abbaszadegan MR. Molecular signaling in tumorigenesis of gastric cancer. *Iran Biomed J*. 2018;22:217-230.
7. Gao J, Liu X, Yang F, Liu T, Yan Q, Yang X. By inhibiting Ras/Raf/ERK and MMP-9, knockdown of EpCAM inhibits breast cancer cell growth and metastasis. *Oncotarget*. 2015;6:27187-27198.
8. Binshtok U, Sprinzak D. The Domino effect in EGFR-ERK signaling. *Dev Cell*. 2018;46:128-130.
9. Wee P, Wang Z. Regulation of EGFR endocytosis by CBL during mitosis. *Cells*. 2018;7:257.
10. Kumar M, Joshi G, Chatterjee J, Kumar R. Epidermal growth factor receptor and its trafficking regulation by acetylation: implication in resistance and exploring the newer therapeutic avenues in cancer. *Curr Top Med Chem*. 2020;20:1105-1123.
11. Breiding DE, Sverdrup F, Grossel MJ, Moscufo N, Boonchai W, Androphy EJ. Functional interaction of a novel cellular protein with the papillomavirus E2 transactivation domain. *Mol Cell Biol*. 1997;17:7208-7219.
12. Spain BH, Bowdish KS, Pacal AR, et al. Two human cDNAs, including a homolog of Arabidopsis FUS6 (COP11), suppress G-protein- and

mitogen-activated protein kinase-mediated signal transduction in yeast and mammalian cells. *Mol Cell Biol*. 1996;16:6698-6706.
13. Jin DY, Teramoto H, Giam CZ, Chun RF, Gutkind JS, Jeang KT. A human suppressor of c-Jun N-terminal kinase 1 activation by tumor necrosis factor alpha. *J Biol Chem*. 1997;272:25816-25823.
14. Cardamone MD, Tanasa B, Cederquist CT, et al. Mitochondrial retrograde signaling in mammals is mediated by the transcriptional cofactor GPS2 via direct mitochondria-to-nucleus translocation. *Mol Cell*. 2018;69:757-772.e757.
15. Drareni K, Ballaire R, Barilla S, et al. GPS2 deficiency triggers maladaptive white adipose tissue expansion in obesity via HIF1A activation. *Cell Rep*. 2018;24:2957-2971.e2956.
16. Fan R, Toubal A, Goni S, et al. Loss of the co-repressor GPS2 sensitizes macrophage activation upon metabolic stress induced by obesity and type 2 diabetes. *Nat Med*. 2016;22:780-791.
17. Zhang J, Kalkum M, Chait BT, Roeder RG. The N-CoR-HDAC3 nuclear receptor corepressor complex inhibits the JNK pathway through the integral subunit GPS2. *Mol Cell*. 2002;9:611-623.
18. Cardamone MD, Krones A, Tanasa B, et al. A protective strategy against hyperinflammatory responses requiring the nontranscriptional actions of GPS2. *Mol Cell*. 2012;46:91-104.
19. O'Meara E, Stack D, Phelan S, et al. Identification of an MLL4-GPS2 fusion as an oncogenic driver of undifferentiated spindle cell sarcoma in a child. *Genes Chromosom Cancer*. 2014;53:991-998.
20. Liu PF, Xiang YC, Liu XW, et al. Cucurbitacin B induces the lysosomal degradation of EGFR and suppresses the CIP2A/PP2A/Akt signaling axis in gefitinib-resistant non-small cell lung cancer. *Molecules*. 2019;24:647.
21. Livak KJ, Schmittgen TD. Analysis of relative gene expression data using real-time quantitative PCR and the 2(-Delta Delta C(T)) method. *Methods*. 2001;25:402-408.
22. Ma WJ, Xiang YC, Yang R, et al. Cucurbitacin B induces inhibitory effects via the CIP2A/PP2A/C-KIT signaling axis in t(8;21) acute myeloid leukemia. *J Pharmacol Sci*. 2019;139:304-310.
23. Xiang Y-C, Shen J, Si Y, et al. Paris saponin VII, a direct activator of AMPK, induces autophagy and exhibits therapeutic potential in non-small-cell lung cancer. *Chin J Nat Med*. 2021;19:195-204.
24. Xu J, Chen Y, Yang R, et al. Cucurbitacin B inhibits gastric cancer progression by suppressing STAT3 activity. *Arch Biochem Biophys*. 2020;684:108314.
25. Zhang Y, Huang P, Liu X, et al. Polyphyllin I inhibits growth and invasion of cisplatin-resistant gastric cancer cells by partially inhibiting CIP2A/PP2A/Akt signaling axis. *J Pharmacol Sci*. 2018;137:305-312.
26. Si Y, Wang J, Liu X, et al. Ethoxysanguinarine, a novel direct activator of AMP-activated protein kinase, induces autophagy and exhibits therapeutic potential in breast cancer cells. *Front Pharmacol*. 2019;10:1503.
27. Khanna A, Bockelman C, Hemmes A, et al. MYC-dependent regulation and prognostic role of CIP2A in gastric cancer. *J Natl Cancer Inst*. 2009;101:793-805.
28. Meric-Bernstam F, Johnson AM, Dumbrava EEI, et al. Advances in HER2-targeted therapy: novel agents and opportunities beyond breast and gastric cancer. *Clin Cancer Res*. 2019;25:2033-2041.
29. Wu SG, Shih JY. Management of acquired resistance to EGFR TKI-targeted therapy in advanced non-small cell lung cancer. *Mol Cancer*. 2018;17:38.
30. Wang Y, Le WD. Autophagy and ubiquitin-proteasome system. *Adv Exp Med Biol*. 2019;1206:527-550.
31. Shrestha N, Shrestha H, Ryu T, et al. δ-Catenin increases the stability of EGFR by decreasing c-Cbl interaction and enhances EGFR/Erk1/2 signaling in prostate cancer. *Mol Cells*. 2018;41:320-330.
32. Yokouchi M, Kondo T, Houghton A, et al. Ligand-induced ubiquitination of the epidermal growth factor receptor involves the interaction of the c-Cbl RING finger and UbcH7. *J Biol Chem*. 1999;274:31707-31712.
33. Sooro MA, Zhang N, Zhang P. Targeting EGFR-mediated autophagy as a potential strategy for cancer therapy. *Int J Cancer*. 2018;143:2116-2125.
34. Ma WB, Wang XH, Li CY, et al. GPS2 promotes erythroid differentiation by control of the stability of EKLF protein. *Blood*. 2020;135:2302-2315.
35. Lentucci C, Belkina AC, Cederquist CT, et al. Inhibition of Ubc13-mediated ubiquitination by GPS2 regulates multiple stages of B cell development. *J Biol Chem*. 2017;292:2754-2772.
36. Huang XD, Xiao FJ, Wang SX, et al. G protein pathway suppressor 2 (GPS2) acts as a tumor suppressor in liposarcoma. *Tumour Biol*. 2016;37:13333-13343.
37. Chan S, Smith E, Gao Y, et al. Loss of G-protein pathway suppressor 2 promotes tumor growth through activation of AKT Signaling. *Front Cell Dev Biol*. 2020;8:608044.
38. Arienti C, Pignatta S, Tesei A. Epidermal growth factor receptor family and its role in gastric cancer. *Front Oncol*. 2019;9:1308.
39. Li X, Wu C, Chen N, et al. PI3K/Akt/mTOR signaling pathway and targeted therapy for glioblastoma. *Oncotarget*. 2016;7:33440-33450.
40. Wang T, Yang J, Xu J, et al. CHIP is a novel tumor suppressor in pancreatic cancer through targeting EGFR. *Oncotarget*. 2014;5:1969-1986.
41. Sorkina T, Bild A, Tebar F, Sorkin A. Clathrin, adaptors and eps15 in endosomes containing activated epidermal growth factor receptors. *J Cell Sci*. 1999;112(Pt 3):317-327.
42. Caldieri G, Barbieri E, Nappo G, et al. Reticulon 3-dependent ER-PM contact sites control EGFR nonclathrin endocytosis. *Science (New York, NY)*. 2017;356:617-624.
43. Capuani F, Conte A, Argenzio E, et al. Quantitative analysis reveals how EGFR activation and downregulation are coupled in normal but not in cancer cells. *Nat Commun*. 2015;6:7999.
44. Henson E, Chen Y, Gibson S. EGFR family members' regulation of autophagy is at a crossroads of cell survival and death in cancer. *Cancers*. 2017;9:27.
45. Fraser J, Simpson J, Fontana R, Kishi-Itakura C, Ktistakis NT, Gammoh N. Targeting of early endosomes by autophagy facilitates EGFR recycling and signalling. *EMBO Rep*. 2019;20:e47734.

SUPPORTING INFORMATION

Additional supporting information may be found in the online version of the article at the publisher's website.

How to cite this article: Si Y, Zhang H, Peng P, et al. G protein pathway suppressor 2 suppresses gastric cancer by destabilizing epidermal growth factor receptor. *Cancer Sci*. 2021;112:4867–4882. doi:10.1111/cas.15151